Virtual metrology frame technique for improving dynamic performance of a small size machine tool

Jonathan Abir [a,*], Stefano Longo [b], Paul Morantz [c], and Paul Shore [d,e]

[a] *The Precision Engineering Institute, School of Aerospace, Transport and Manufacturing, Cranfield University, Cranfield, MK43 0AL, UK (e-mail: j.h.abir@cranfield.ac.uk).*

[b] *The Centre for Automotive Engineering and Technology, Cranfield University, Cranfield, MK43 0AL, UK (e-mail: s.longo@cranfield.ac.uk)*

[c] *The Precision Engineering Institute, School of Aerospace, Transport and Manufacturing, Cranfield University, Cranfield, MK43 0AL, UK (e-mail: P.Morantz@cranfield.ac.uk).*

[d] *The National Physical Laboratory, Teddington, TW11 0LW, UK (e-mail: paul.shore@npl.co.uk)*

[e] *The Precision Engineering Institute, School of Aerospace, Transport and Manufacturing, Cranfield University, Cranfield, MK43 0AL, UK.*

Abstract

This paper presents a novel concept, a virtual metrology frame, for enhancing the dynamic performance of a machine tool with a flexible structural frame. The dynamic properties of a machine are directly affected by the stiffness of its frame, and its reference system; thus, by having an unstressed metrology frame, superior dynamic capabilities can be achieved. The developed concept does not require physical components associated with metrology frame; hence it is ideal for machine tools with requirements for small footprint and ultra-precision performance. The concept relies on an accelerometer based dynamic displacement feedback technique, where the accelerometer is used as a precision frame displacement sensor. The concept does not require a complex controller, and was realized in an off-the-shelf CNC controller. The concept was demonstrated on a linear motion system, a simplified version of a compact size CNC machine, and its servo bandwidth and dynamic stiffness were improved by 36 % and 70 % respectively, which are the key parameters for improving the machining accuracy.

Keywords: acceleration based displacement, flexible frame, PID controller, sensitivity function, virtual metrology frame.

1 Introduction

Reduction of machining error enables higher dimension accuracy in Computerized Numerical Control (CNC) machines. The significant fraction (90%) of machining error is cause by dynamic positioning error in a machine tool servo [1]; this positioning error results in a contour error on the machined part. In Proportional-Integral-Derivative (PID) type servo controllers, the most common controller used in industrial CNCs [2], tracking error contributes to error in position; tracking error occurs in a closed-loop control system due to an inability to follow rapidly varying position commands [3]. This error can be reduced by increasing feedback gains and servo bandwidth [4–7]; however, the amounts by which these parameters can be increased are limited by sensitivity to measurement noise and mechanical resonance excitation, respectively [4,7,8].

There are three important types of mechanical resonances that can limit machine dynamics [9]: actuator flexibility, guiding system flexibility, and frame flexibility. Actuator flexibility occurs when there is compliance between the motor and the load, typically where there is a gear in the system. Guiding system flexibility occurs when the driving force is not coincident with the center of gravity and stiffness is limited. Frame flexibility occurs due to servo-reaction forces causing dynamic deformation, resulting in frame resonance excitation i.e. a stressed frame. The problem of servo control limited by mechanical resonance in machine tools is well studied in literature, most references focus on actuator flexibility; few papers describe the problem of flexible frames [10–13].

Notch filtering is commonly used in industry to attenuate mechanical resonances in the control signal [14]; however this reduces the drives' bandwidths, limiting its application in improving machine tool performance [15].

Pre-filtering trajectory techniques can be used to reduce machine structure excitation [16], however their implementation is challenging [8]. Impulse/jerk decoupling technology [17,18] utilizes a mechanical low-pass filter, which adds another degree of freedom to the system. An expansion to this technology, which is often used in the lithographic industry, is a dual stage motion system [19,20]. In this concept a fine short stroke motor with ultraprecision positioning is mounted to a coarse driving mechanism; however, this concept is complex and requires additional sensors, actuators, volume, and cost.

Acceleration feedback was used for damping structural resonances [16,21,22]; by adding acceleration feedback to the position control loop, as an inner feedback loop, the disturbance force experiences a virtually larger mass, improving the process sensitivity [23]. Process dynamics, controller calculation delay, and accelerometer roll-off result in instability. Reducing the acceleration loop gain for higher frequencies counteract this instability; however to maintain position loop stability margins the acceleration loop requires a high bandwidth [21,24]. Controllers in industrial feed drives commonly use position feedback only, since other movement variables are not available [16,21], this limits acceleration feedback realization in commercial CNC. Acceleration can be measured directly by an accelerometer, calculated from the second derivative of position measurements, or by observer techniques. Using accelerometer provides absolute acceleration measurement; however, both rigid

body and structural vibrations are mixed in the signal. Differentiation of position signal produces quantization noise [25], passing this signal through filters limits the closed loop control performance [26]. Acceleration observers offers lower noise content than differentiation, however these are limited by parameter dependence [26,27].

The position signal in a linear motion system is typically provided by a linear encoder which is generally located at the machine frame; hence, deformation in flexible elements anywhere between the encoder scale and the point to be controlled is not compensated [28]. In [29] an accelerometer located close to the Tool Center Point (TCP) is used. The TCP position is estimated by a state space observer, and used as position feedback, improving dynamic behavior; however, this implementation is non-trivial due to the non-collocated control [22]. In [8] a model-based control is used to estimate the machine frame deformation with respect to the TCP, where no additional drive is required; however, frequency and damping of structural modes may vary over time, and also as a function of machine configuration [16].

This paper addresses the problem of frame flexibility, which is often neglected in the design stage, thus leading to unexpected problems during the prototype test phase [10]. A virtual metrology frame technique was developed to achieve high dynamic performance as though the machine has a separate stiff metrology frame, by measuring machine frame displacement using an acceleration sensor. The developed technique was implemented on a commercial PID controller, while other structural resonance compensation techniques cannot be applied in commercial CNC systems [30].

2 Virtual metrology frame concept

The Virtual Metrology Frame (VMF) concept was designed to improve the performance of a machine with flexible frame phenomena that limit performance. The dynamic properties of the machine are directly affected by the stiffness of the frame and its reference system. By utilizing an unstressed metrology frame, superior dynamic capabilities can be achieved [10,19,31,32].

The VMF concept is realized (Fig. 1a) by distinguishing between the carriage position, with respect to the stressed frame X_c, and the frame displacement due to flexible modes X_f; hence, an unperturbed position signal X_{vmf} can be obtained in the presence of these frame flexible modes. A typical PID controller structure C can be applied using the VMF (Fig. 1b). A reference position signal X_{set} is fed into the controller C, with output u, the control signal. The plant P is the system to be controlled, it has input u, and output X_c measured by a position sensor, typically a linear encoder; however, in the VMF concept a second output to the plant X_f, the frame displacement, is added to X_c within the controller; thus, the controlled position signal X_{vmf} is the sum of the position measurement signals, enabling attenuation of the machine frame resonance.

In a system with a flexible frame, there are two possible plant Transfer Functions (TFs): P_c (1) and P_{vmf} (2) depending on the carriage position signal X_c and X_{vmf} respectively, where m_c and m_f are the carriage and the frame mass respectively and k_f is the frame stiffness. The P_c consists of two modes: a carriage rigid body mode and a flexible frame mode. In the P_{vmf}, there is only carriage rigid

body mode. In a system with an infinite frame stiffness, the flexible frame mode is negligible and $P_c \approx P_{vmf}$. The Bode diagram of the plant TFs is shown in Fig. 2; the P_{vmf} is a double integrator type while P_c is Antiresonance-Resonance type [9]. In practice, P_c may contain multiple flexible frame modes while P_{vmf} may not completely attenuate these modes.

$$P_c(s) = \frac{X_c(s)}{F(s)} = \frac{1}{m_c s^2} + \frac{1}{m_f s^2 + k_f} \tag{1}$$

$$P_{vmf}(s) = \frac{X_{vmf}(s)}{F(s)} = \frac{1}{m_c s^2} \tag{2}$$

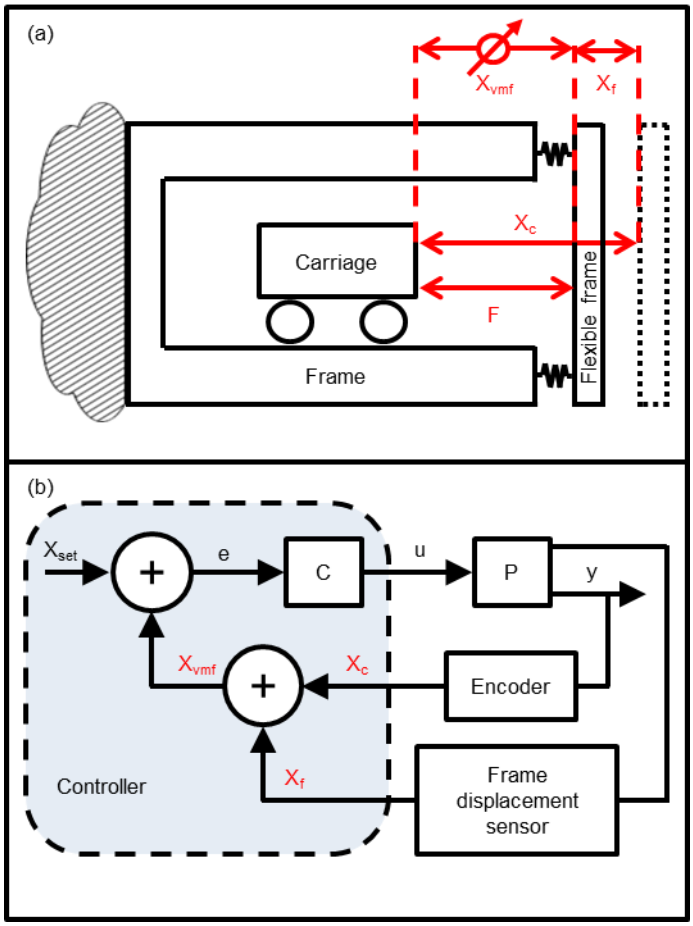

Figure 1. The Virtual Metrology Frame (VMF) concept.

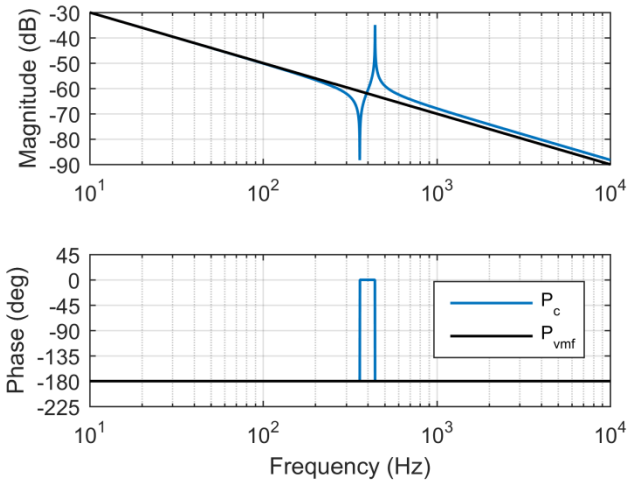

Figure 2. Plant Transfer Functions (TFs). P_c and P_{vmf} are the plant TFs where the position signal is X_c and X_{vmf} respectively.

The VMF concept does not require physical components associated with a metrology frame, hence it is ideal for a compact size machine tool with the requirement for small footprint [33,34] and ultra-precision performance [35,36]. Furthermore, this concept is very suitable for industrial deployment as it allows implementation within an off-the-shelf controller without modification. The concept was simply implemented in a PID controller, which is the most common controller found in industrial machine tools [2,5,37].

The VMF concept relies on real-time measurement of the frame displacement – "frame displacement sensor" (Fig. 1b). Common techniques for precision displacement sensors require a fixed reference system [38,39], i.e. a secondary physical frame. A unique frame displacement measurement technique using accelerometers was developed [40], which offers a superior solution without a secondary physical frame. The accelerometer measures the acceleration of a point without a fixed reference system; thus, by double integration the frame displacement X_f can be estimated relative to its "unstressed state" (Fig. 1a).

The VMF concept uses an accelerometer to measure frame displacement, thus it differs from acceleration feedback techniques as no special inner loop, i.e. acceleration feedback, is required; hence no special technique is required to tune the controller gains. Furthermore, the technique offers wideband frame resonances attenuation, and there is no "targeted" resonance to attenuate as in other common techniques [14].

The frame displacement signal X_f and the carriage position signal X_c are complementary (Fig. 1a)

$$X_c = X_{vmf} + X_f \ . \tag{3}$$

The controller update rate is significantly lower than the encoder and frame displacement sensor update rates, thus the position feedback register (in the controller) is simply their sum according to (3) ; and no special sensors fusion technique is required.

2.1 Frame displacement sensor

Double integration of a signal is a straightforward task; however, integrating noise leads to an output that has a Root Mean Square (RMS) value that increases over integration time [41], which occurs even in the absence of accelerometer motion. A heave filter H_{est} (4) was used as a displacement estimator [42,43], which is a combination of a High Pass Filter (HPF) and double integrator. A pole-zero placement filter was added to correct phase delay as if the estimator is an ideal double integrator H_{dbl} (5).

$$H_{est} = \frac{s^2}{(s^2 + 2\varsigma \cdot \omega_c \cdot s + \omega_c{}^2)^2} \cdot K \frac{s - z}{s - p} \ , \tag{4}$$

$$H_{dbl} = \frac{1}{s^2} \ , \tag{5}$$

where s is the Laplace variable, ς the damping coefficient, ω_c the cut-off frequency of the filter, p and z are the pole-zero pair where $z < p < 0$ [40], and K is an additional gain parameter. Fig. 3 shows a comparison of Bode plots of the estimator and double integrator. Below the cut-off frequency ($< \omega_c$) the estimator acts as an HPF, while above the cut-off frequency ($> \omega_c$) it acts as a double integrator.

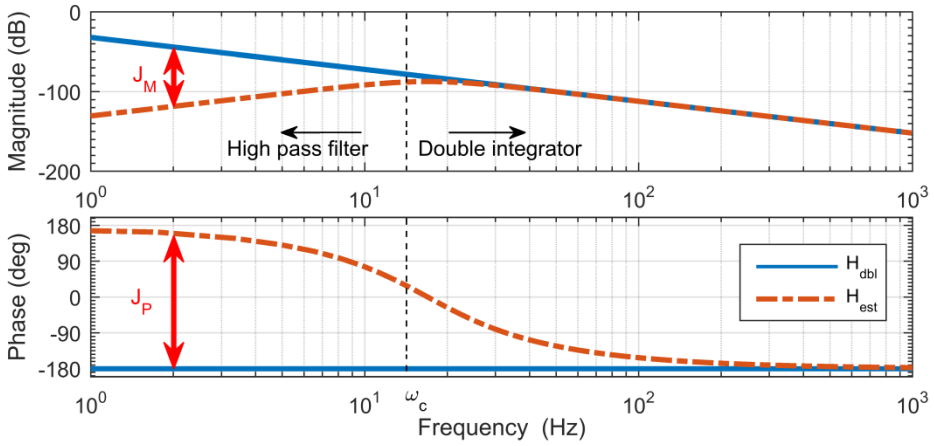

Figure 3. Bode plot of displacement estimator H_{est} and ideal double integrator H_{dbl}. J_M and J_P are the magnitude and phase errors of the estimator.

Real-time implementation of acceleration based displacement measurement in a control system has two main conflicting requirements: small phase error J_P and low displacement noise J_σ; thus, it is rarely reported [44], especially for long term (> 10 s) and accurate (< 0.1 µm) measurements [45].

The estimator was constrained to measure only dynamic displacement of the machine frame that occurs at flexible resonances frequencies ($> \omega_c$); hence it optimize: the displacement noise J_σ, phase error J_P, and magnitude error J_M resulting from double integration of, and HPF application to, the acceleration signal [40].

3 Experimental setup

The µ4 is a small size CNC machine with 6 axes which was conceived in 2008 by Cranfield University [36]. In order to reduce the machine footprint and ease manufacturing, the design was based on modules with common design and simple interfaces; thus, the machine motion axes were split into two near identical modules. Each module consists of at least one rotary, and one linear motions made by direct drive motors (Fig. 4).

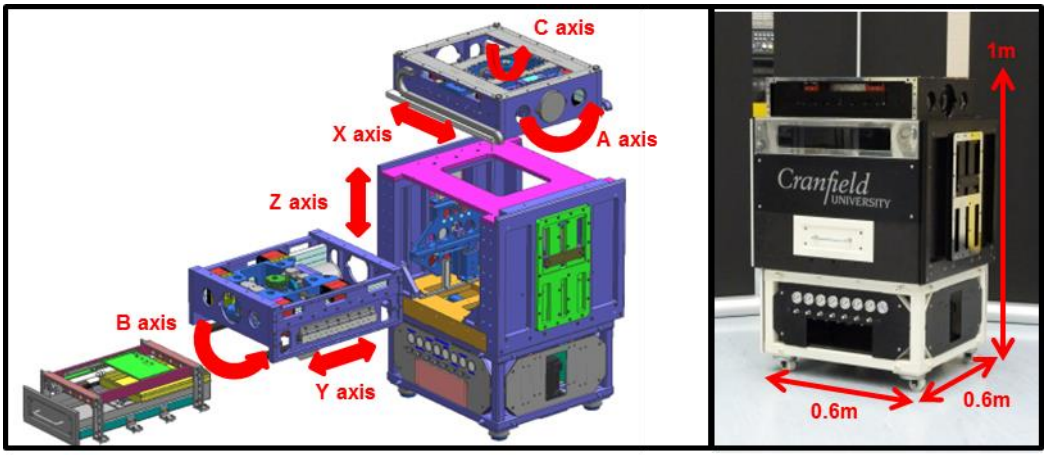

Figure 4. The µ4 machine.

A simplified linear motion module [46], which represents one of the machine motion modules, consisting of: frame, air-bearings, linear motor, linear encoder, and carriage, was used for this study (Fig. 5). The driving force and the position sensor were not applied at the center of gravity but on the "master side", thus, the carriage movement is dependent on the high stiffness of the air-bearings, which suppresses motion in an undesired direction. The carriage and the frame mass are m_c = 17 kg and m_f = 24 kg respectively.

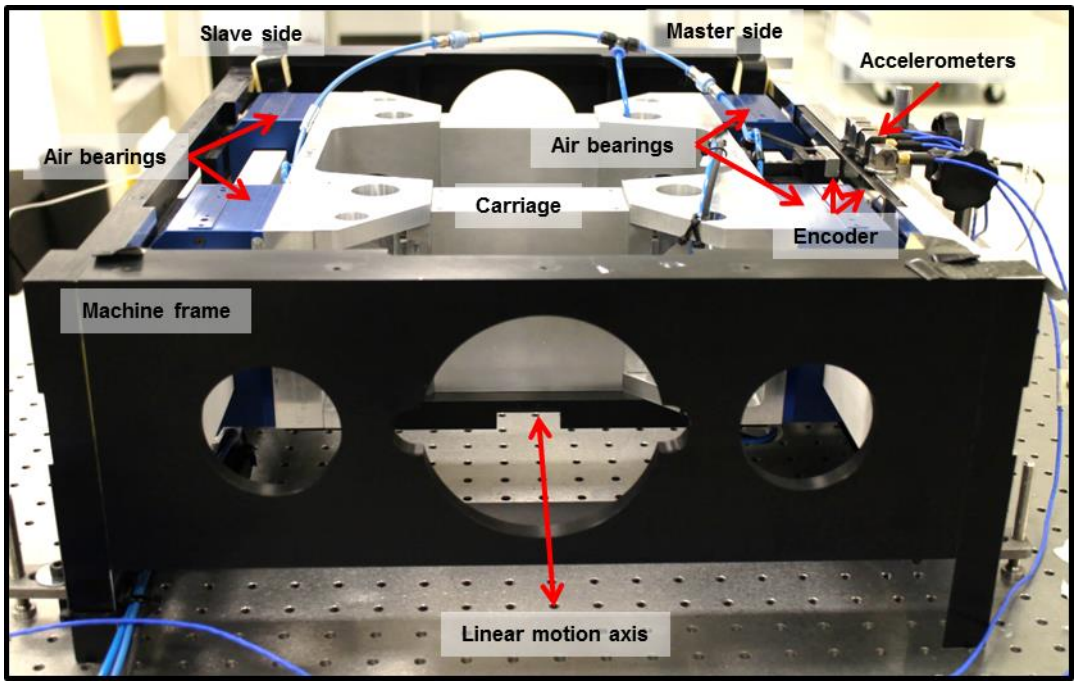

Figure 5. A simplified linear motion module.

A software-based machine controller (Aerotech A3200) was used to control the motion system with a linear digital amplifier (Aerotech Ndrive ML). The digital servo amplifier has a current loop update rate of 50 µs, servo loop update rate of 125 µs, and a tunable PID digital control loop. The frame displacement sensor was connected to the auxiliary analogue input of the drive amplifier. Its update rate was equivalent to the servo update rate. Summation of the encoder and frame displacement signals was implemented in the controller (Fig. 1b).

A linear encoder (Renishaw RELM 20U) with 20 µm pitch was used as the position feedback sensor. Using a controller multiplication factor of 65536, the position resolution was 0.30 nm, and sub divisional error was nominally < ±30 nm [47].

System identification techniques [48,49] showed flexible frame characteristics, where a relative movement between the frame and the carriage is measured by the encoder (Fig. 6). These appear as resonances in the plant Frequency Response Function (FRF) as the encoder scale is mounted to the machine frame, while its read-head is mounted to the carriage (Fig. 5).

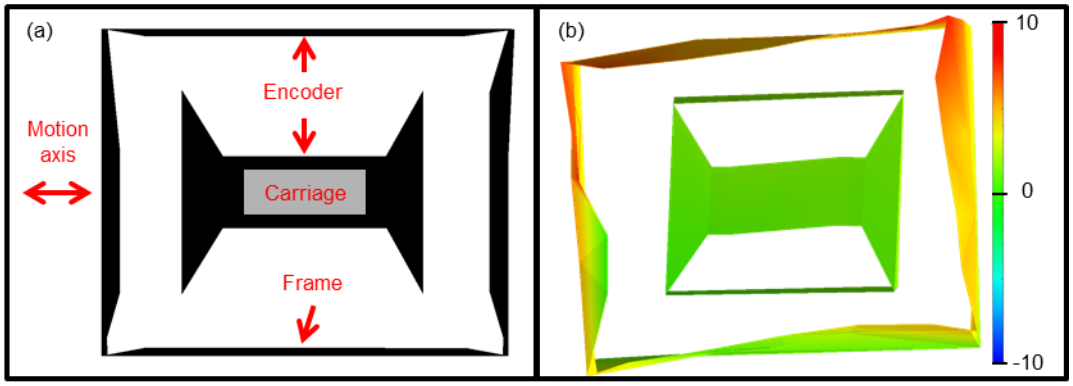

Figure 6. Flexible frame mode shape. Unstressed frame (a), and a flexible frame mode shape (b).

To maintain co-located control, the accelerometer was fixed to the frame as close as possible to the encoder scale (Fig. 7), and aligned with respect to the encoder. The accelerometer location was chosen based on the machine modal analysis [48,49].

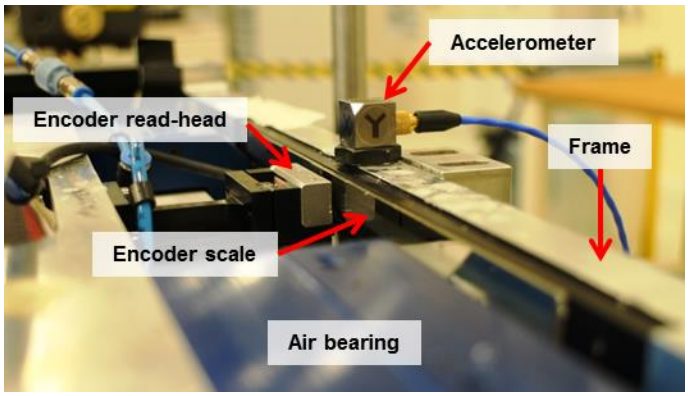

Figure 7. Accelerometer fixed as closed as possible to the encoder scale.

3.1 Frame displacement sensor

The frame displacement sensor was realized using a combination of: an accelerometer, signal conditioner, and an xPC target machine (Fig. 8).

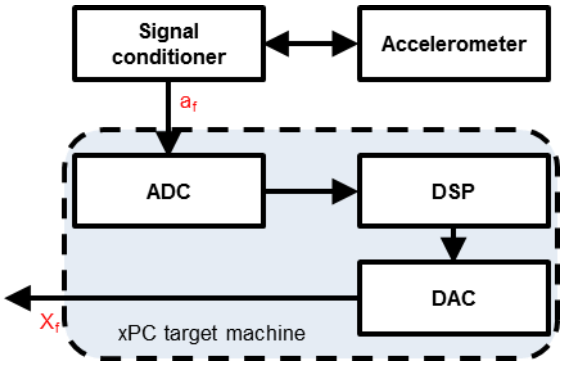

Figure 8. Frame displacement sensor block diagram.

A triaxial ceramic shear Integrated Electronic Piezoelectric (IEPE) general purpose accelerometer (PCB 356A025) was used to determine the frame displacement. The accelerometer sensitivity was 25 mV/g. IEPE accelerometers are the appropriate sensor for low amplitude vibration measurements due to their: low noise; wide dynamic, frequency, and temperature range; high

sensitivity; and availability in small sizes [50]. A low noise signal conditioner was used to power the IEPE accelerometer, and to decouple the acceleration signal (PCB 482C15). The signal conditioner has a typical phase distortion of ±1°.

The xPC target machine (Speedgoat performance) was used for Digital Signal Processing (DSP) with an update rate of 18 µs. It contains 16 bit Analogue Digital Converter (ADC) and Digital to Analogue Converter (DAC). The conversion time for the ADC and DAC is 5 µs and 3 µs, respectively. The xPC target machine is optimized for MathWorks® SIMULINK® and xPC Target™.

The frame displacement sensor has time delay τ_{fds}. It is composed of accelerometer delay τ_{acc}, DSP delay τ_{DSP}, and estimator delay τ_{est}. The accelerometer delay is frequency dependent, and specified by the accelerometer manufacturer. The DSP delay is due to the time it takes to read and process the accelerometer signal, and therefore dependent on the computing power available. The frame displacement sensor delay τ_{fds}, which is the sum of its components delays, must be smaller than the controller update rate τ_{servo}, to allow resonance attenuation:

$$0.5 \cdot \tau_{servo} > \tau_{fds} = \left| \tau_{acc} + \tau_{est} + \tau_{DSP} \right| . \quad (6)$$

The frame displacement sensor delay, based on an optimized displacement estimator, is shown in Fig. 9.

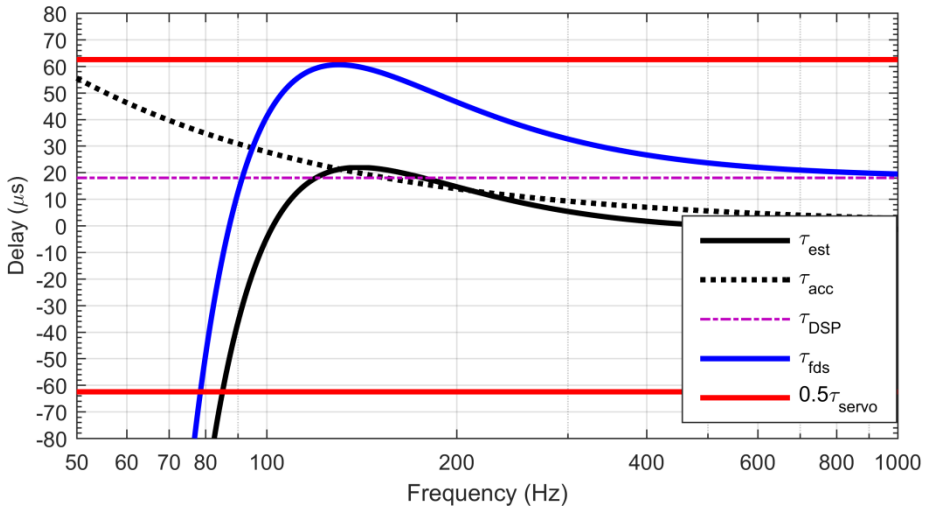

Figure 9. Frame displacement sensor time delay. Accelerometer delay τ_{acc}, DSP delay τ_{DSP}, estimator delay τ_{est}, frame displacement sensor delay τ_{fds}, and the controller update rate τ_{servo}.

The frame displacement sensor was validated against a laser interferometer (Renishaw ML10 gold standard) [40] and capacitance sensors (Lion precision PX405HC) [42,43]. Displacement noise was σ < 30 nm over 10 minutes of measurement [40].

4 Proportional-Integral-Derivative controller tuning

The controller was composed of a PID filter, second order Low Pass Filter (LPF), and a Bi-quad filter, as in (7)-(9). The LPF and Bi-quad filter were designed to terminate the PID differentiating action and reduce multiple high-frequency resonances.

$$H_{pid}(s) = \frac{K}{s}[(T_D s + 1) \cdot (s + \frac{1}{T_I})], \tag{7}$$

$$H_{lpf}(s) = \frac{(2\pi f_{lp})^2}{s^2 + 2\zeta_{lp} \cdot (2\pi f_{lp}) \cdot s + (2\pi f_{lp})^2} \ , \tag{8}$$

$$H_{bq}(s) = \frac{s^2 + 2\zeta_n \cdot (2\pi f_n) \cdot s + (2\pi f_n)^2}{s^2 + 2\zeta_d \cdot (2\pi f_d) \cdot s + (2\pi f_d)^2} \ . \tag{9}$$

where K is the proportional gain and T_I and T_D are the integral and derivative time respectively; ζ_{lp} and f_{lp} are the LPF damping ratio and frequency respectively; f_n and f_d are the Bi-quad filter zero and pole frequencies respectively, and ζ_n and ζ_d are their damping ratios.

The Phase Margin (PM) ϕ_m and Gain Margin (GM) G_m relate servo drive stability to control design parameters. In order to maintain machine tool stability the PM and GM values should be [51,52]:

$$\phi_m \geq 45^\circ \ , \tag{10}$$

$$G_m \geq 6 \ dB \ . \tag{11}$$

A Matlab control system tuning toolbox was used to tune and optimise the controller by using nonsmooth optimisation algorithms [53], and computes the H_∞ norm using the algorithm detailed in [54]. The PM and GM tuning goals were set according to (10) and (11) respectively. The first gain crossover of the open loop FRF f_s, and overshoot M_p constraints were set according to (12) and (13), respectively.

$$10 \text{ Hz} \leq f_s \leq 100 \text{ Hz} \ , \tag{12}$$

$$M_p \leq 25 \ \% \ . \tag{13}$$

5 Results

This section shows the experimental results validating the VMF concept, and comparison of the optimized controller with and without the VMF concept.

5.1 Validation of the virtual metrology frame concept

The VMF concept was realized by connecting the xPC target machine output X_f to the machine controller. Summation of the two signals in the controller was set to the maximum update rate – the servo update rate of 125 µs.

Using sinusoidal excitation the machine plant Transfer Function (TF) was measured. Comparison of the plant TFs with and without the VMF is shown in Fig. 10. A significant magnitude reduction of 12 dB in the frame's first resonance can be observed. Furthermore, the VMF has been shown to be a wide bandwidth resonance attenuation technique. The second resonance shows no attenuation by this setup as its mode shape produced a non-collinear displacement to the measured axis; this second resonance causes a relative movement between the encoder read-head and scale

which is measured as displacement and appears as a resonance, while the frame displacement sensor measures only collinear displacement to the measured axis.

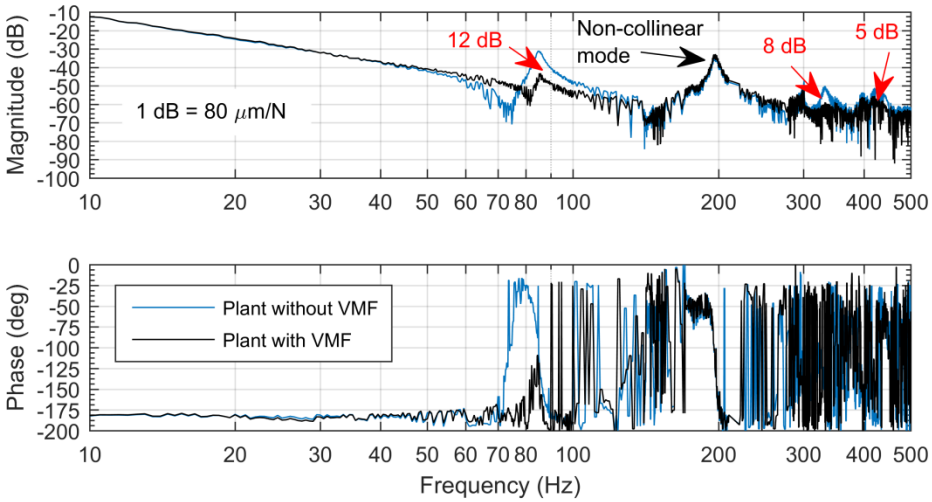

Figure 10. Plant Transfer Functions (TFs) with and without the Virtual Metrology Frame (VMF) concept.

5.2 Optimized controller

A PID controller (Section 4) was designed and optimized based on curve fitted plant TFs with and without the VMF (Fig. 9); a 'peak picking' curve fitting method [55] was used to curve fit the measured plant TFs. A Bi-quad filter (9) was used to attenuate the machine second resonance, with the following parameters: ζ_n = 0.0175, ζ_d = 0.2156, and $f_n = f_d$ = 198 Hz. The optimization results of the PID filter gains are shown in Table 1. To aid in the comparison between the two optimized controllers, a vector margin stability criteria M_s was used [56]. Because the vector margin is a single margin parameter, it removes all the ambiguities in assessing stability using gain and phase margins.

Table 1. Optimized PID controllers parameters. K, T_I, and T_D are the PID proportional gain, integral time and derivative time respectively. f_{lp} and ζ_{lp} are the LPF cut-off frequency and damping parameters, respectively. M_p is the closed loop overshoot and f_s is the open loop crossover frequency. ϕ_m, G_m, and M_s are the phase, gain, and vector margin respectively.

	K	T_I [s]	T_D [s]	f_{lp} [Hz]	ζ_{lp}	f_s [Hz]	M_p [%]	ϕ_m [deg]	G_m [dB]	M_s [dB]
System without VMF	$3.28 \cdot 10^4$	0.08	0.04	189.67	0.67	22.20	18.14	59.75	15.95	2.75
System with VMF	$5.61 \cdot 10^4$	0.10	0.03	166.63	0.85	30.19	16.71	62.33	18.81	2.59

Implementing the VMF in the control system improved the proportional and derivative gains by 70 % and 38 % respectively, while the overshoot was reduced, and the stability margin remains almost the same (Fig. 11), thus, the open loop crossover frequency, i.e. servo bandwidth, was improved by 36 %. The open loop Nyquist and Bode plots with and without the VMF concept are shown in Fig. 11 and 12.

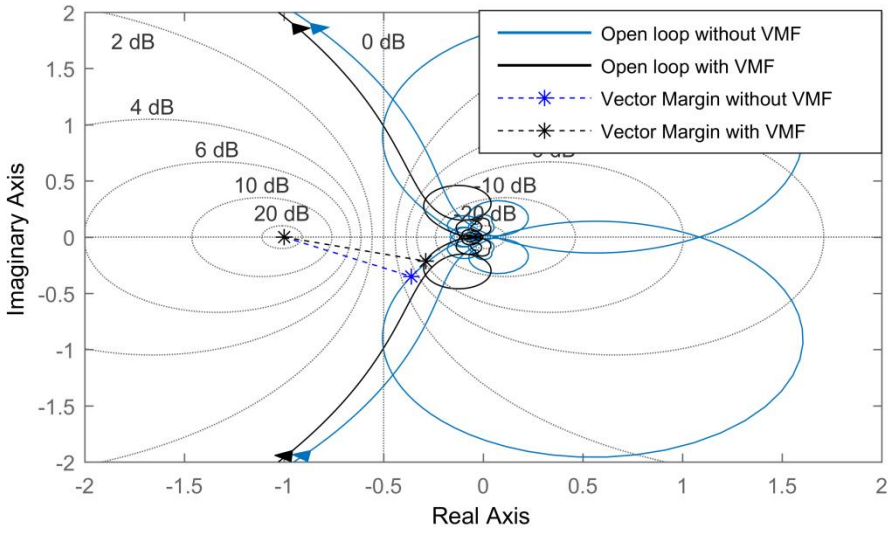

Figure 11. Open loop Nyquist plot with and without the Virtual Metrology Frame (VMF) concept.

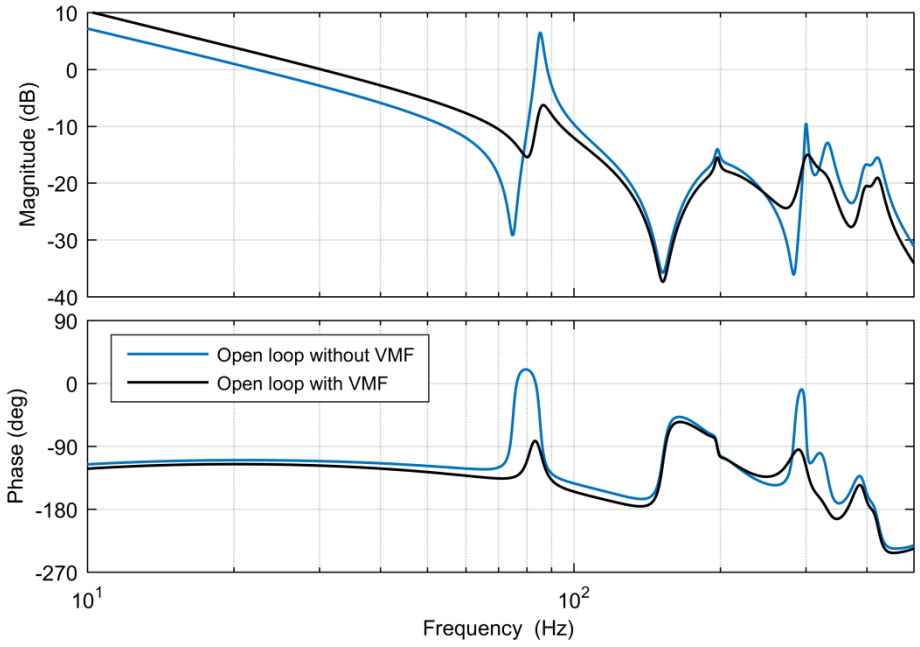

Figure 12. Open loop Bode plot with and without the Virtual Metrology Frame (VMF) concept.

Three sensitivity functions determine the feedback error of the system: sensitivity function $S(s)$, complementary sensitivity function $T(s)$, and process sensitivity function $PS(s)$ [57]: these functions represent the ability of the feedback system to reject disturbances acting on the output of the system; the system response to the reference in case X_{set}=1; and the machine dynamic compliance respectively. The sensitivity functions with and without the VMF are shown in Fig. 13. When the VMF was applied, the machine dynamic stiffness (inverse process sensitivity) and sensitivity function were shown to be equivalent to the improved proportional gain.

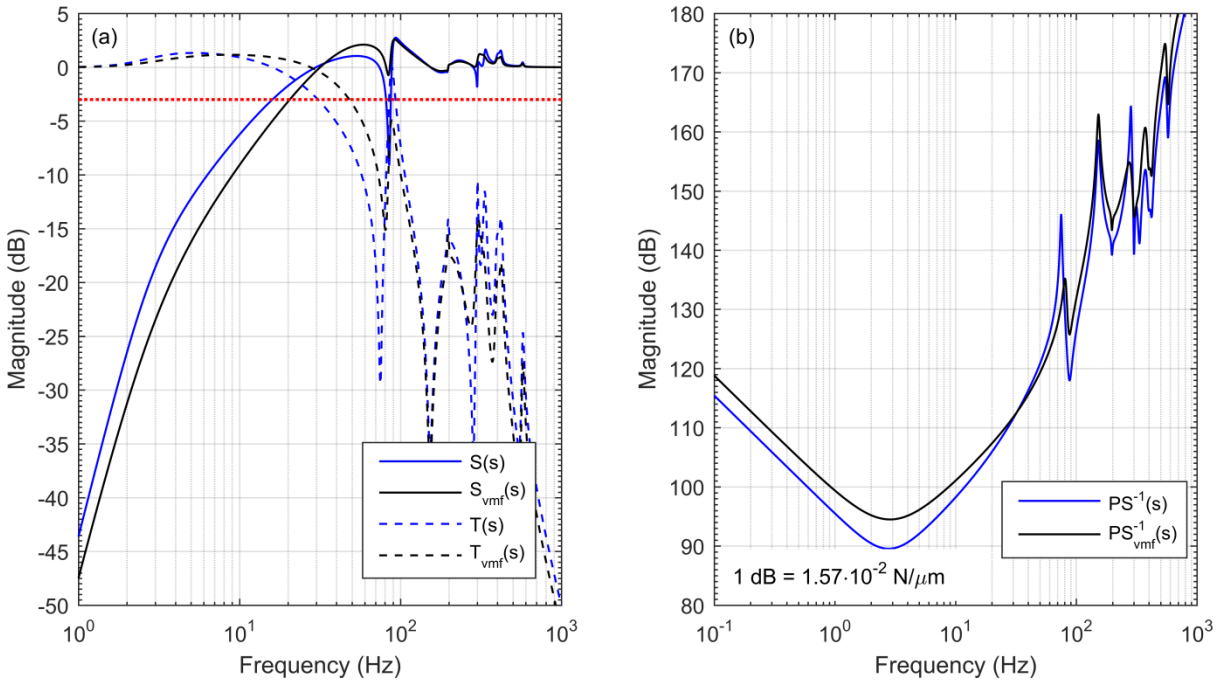

Figure 13. Sensitivity functions. $S(s)$, $T(s)$, and $PS^{-1}(s)$ are the machine sensitivity, complementary sensitivity and inverse process sensitivity functions respectively. $S_{vmf}(s)$, $T_{vmf}(s)$, and $PS^{-1}{}_{vmf}(s)$ are the machine with the virtual metrology frame sensitivity, complementary sensitivity and inverse process sensitivity functions respectively.

6 Conclusions

The Virtual Metrology Frame is a servo plant compensation technique to address frame flexibility. It offers a solution of enhancing machine performance utilizing a virtual metrology system, without a physical metrology frame. The developed concept is insensitive to plant frequency changes in contrast with common techniques.

The VMF concept is based on a technique to measure frame displacement without having a fixed reference system. Using bespoke signal processing, an accelerometer was used as a precision positioning (displacement) sensor.

Implementing the VMF concept on the linear motion system, the metrology loop showed superior rigidity; this was due to the virtual separation of the metrology system and the force system. The VMF was designed to measure encoder scale displacement that occurs due to frame flexible modes only; whilst floor vibrations and rigid body modes, which appear in the acceleration signal, are attenuated significantly by the HPF. The VMF concept could be implemented in a multi-axes system, such as CNC machine, for each motion axis independently; hence measuring the position of the carriage (or the tool) relative to the "unstressed state" of the reference frame. The effectiveness of the VMF concept in a multi-axes machine should be addressed in a future study. Furthermore, this technique could also be implemented in rotary axes by using angular accelerometers.

The concept can be implemented in any feedback controller, requiring only a summing of two position signals: encoder and frame displacement; thus it very suitable for industrial deployment. It can be used to improve the performance of an existing machine with minimal retro-fit to the machine. In the future, the Speedgoat controller could be replaced seamlessly by dedicated lower cost electronics, such as a field-programmable gate array (FPGA), and would be connected to the auxiliary analogue input in the controller.

The concept was demonstrated on a simplified motion module of a commercial CNC machine equipped with a PID controller. The flexible frame resonances present in the position signal were attenuated significantly, but not completely. This can be explained by the fact that frame vibrations cause forced vibrations of the carriage; however, a significant improvement to the servo bandwidth and dynamic stiffness were shown, which are key parameters for improving the machining accuracy. These improvements were implemented with no affect upon the system stability.

Acknowledgment

This work was supported by the UK EPSRC under grant EP/I033491/1 and the Centre for Innovative Manufacturing in Ultra-Precision. J. Abir acknowledges the McKeown Precision Engineering and Nanotechnology foundation at Cranfield University, and B'nai B'rith Leo Baeck (London) for their financial support. The authors would like to thank James Norman for comments that improved the manuscript.

References

[1] Chiu G, Tomizuka M. Contouring control of machine tool feed drive systems: a task coordinate frame approach. IEEE Trans Control Syst Technol 2009;9:130–9. doi:10.1109/87.896754.

[2] Kim D, Son DH, Jeon D. Feed-system autotuning of a CNC machining center: Rapid system identification and fine gain tuning based on optimal search. Precis Eng 2012;36:339–48. doi:10.1016/j.precisioneng.2011.09.007.

[3] Altintas Y. Manufacturing automation: metal cutting mechanics, machine tool vibrations, and CNC design. Cambridge university press; 2012. doi:10.1115/1.1399383.

[4] Ramesh R, Mannan MA, Poo AN. Tracking and contour error control in CNC servo systems. Int J Mach Tools Manuf 2005;45:301–26. doi:10.1016/j.ijmachtools.2004.08.008.

[5] Erkorkmaz K, Altintas Y. High speed CNC system design. Part III: High speed tracking and contouring control of feed drives. Int J Mach Tools Manuf 2001;41:1637–58. doi:http://dx.doi.org/10.1016/S0890-6955(01)00004-9.

[6] Pritschow G. On the influence of the velocity gain factor on the path deviation. CIRP Ann - Manuf Technol 1996;45:367–71.

[7] Pritschow G. A Comparison of Linear and Conventional Electromechanical Dives. CIRP Ann - Manuf Technol 1998;47:541–8. doi:http://dx.doi.org/10.1016/S0007-8506(07)63241-7.

[8] Uhlmann E, Eßmann J, Wintering J-HH. Design- and control-concept for compliant machine tools based on controller integrated models. CIRP Ann - Manuf Technol 2012;61:347–50. doi:http://dx.doi.org/10.1016/j.cirp.2012.03.143.

[9] Coelingh E, De Vries TJA, Koster R. Assessment of mechatronic system performance at an early design stage. IEEE/ASME Trans Mechatronics 2002;7:269–79. doi:10.1109/TMECH.2002.803630.

[10] Rankers AM, van Eijk J. The influence of reaction forces on the behaviour of high performance motion systems. Proc. Second Int. Conf. Motion Vib. Control. Yokohama, 1994, p. 711–6.

[11] Weck M, Krüger P, Brecher C. Limits for controller settings with electric linear direct drives. Int J Mach Tools Manuf 2001;41:65–88. doi:10.1016/S0890-6955(00)00063-8.

[12] Lamikiz A, De Lacalle LNL, Celaya A. Machine tools for high performance machining. Springer; 2009. doi:10.1007/978-1-84800-380-4_6.

[13] López J, Artés M, Alejandre I. Analysis of optical linear encoders' errors under vibration at different mounting conditions. Measurement 2011;44:1367–80. doi:10.1016/j.measurement.2011.05.004.

[14] Kamalzadeh A, Erkorkmaz K. Accurate tracking controller design for high-speed drives. Int J Mach Tools Manuf 2007;47:1393–400. doi:http://dx.doi.org/10.1016/j.ijmachtools.2006.08.027.

[15] Altintas Y, Khoshdarregi MR. Contour error control of CNC machine tools with vibration avoidance. CIRP Ann -

Manuf Technol 2012;61:335–8. doi:10.1016/j.cirp.2012.03.132.
[16] Altintas Y, Verl A, Brecher C, Uriarte L, Pritschow G. Machine tool feed drives. CIRP Ann - Manuf Technol 2011;60:779–96. doi:10.1016/j.cirp.2011.05.010.
[17] Brecher C, Wenzel C, Klar R. Characterization and optimization of the dynamic tool path of a highly dynamic micromilling machine. CIRP Ann - Manuf Technol 2008;1:86–91. doi:10.1016/j.cirpj.2008.09.013.
[18] Denkena B, Hesse P, Gümmer O. Energy optimized jerk-decoupling technology for translatory feed axes. CIRP Ann - Manuf Technol 2009;58:339–42. doi:http://dx.doi.org/10.1016/j.cirp.2009.03.043.
[19] Butler H. Position control in lithographic equipment. IEEE Control Syst Mag 2011;31:28–47.
[20] Shinno H, Yoshioka H, Taniguchi K. A Newly Developed Linear Motor-Driven Aerostatic X-Y Planar Motion Table System for Nano-Machining. CIRP Ann - Manuf Technol 2007;56:369–72. doi:http://dx.doi.org/10.1016/j.cirp.2007.05.086.
[21] Butler H. Acceleration feedback in a lithographic tool. Control Eng Pract 2012;20:453–64. doi:10.1016/j.conengprac.2011.12.008.
[22] Munoa J, Beudaert X, Erkorkmaz K, Iglesias A, Barrios A, Zatarain M. Active suppression of structural chatter vibrations using machine drives and accelerometers. CIRP Ann - Manuf Technol 2015;64:385–8. doi:10.1016/j.cirp.2015.04.106.
[23] Ellis G, Lorenz RD. Resonant load control methods for industrial servo drives. Conf Rec 2000 IEEE Ind Appl Conf Thirty-Fifth IAS Annu Meet World Conf Ind Appl Electr Energy 2000;3:1438–45. doi:10.1109/IAS.2000.882073.
[24] Kang J, Chen S, Di X. Online detection and suppression of mechanical resonance for servo system. ICICIP 2012 - 3rd Int. Conf. Intell. Control Inf. Process., 2012, p. 16–21. doi:10.1109/ICICIP.2012.6391515.
[25] Pritschow G, Eppler C, Lehner W-D. Ferraris Sensor – The Key for advanced dynamic Drives. CIRP Ann - Manuf Technol 2003;52:289–92. doi:10.1016/S0007-8506(07)60586-1.
[26] Han JD, Wang YC, Tan DL, Xu WL. Acceleration feedback control for direct-drive motor system. Proc. IEEE/RSJ Int. Conf. Intell. Robot. Syst. (IROS 2000), vol. 2, IEEE; 2000, p. 1068–74. doi:10.1109/IROS.2000.893161.
[27] Moatemri MH, Schmidt PB, Lorenz RD. Implementation of a DSP-based, acceleration feedback robot controller: practical issues and design limits. Conf. Rec. 1991 IEEE Ind. Appl. Soc. Annu. Meet., IEEE; 1991, p. 1425–30. doi:10.1109/IAS.1991.178047.
[28] Kono D, Matsubara A, Nagaoka K, Yamazaki K. Analysis method for investigating the influence of mechanical components on dynamic mechanical error of machine tools. Precis Eng 2012;36:477–84. doi:10.1016/j.precisioneng.2012.02.006.
[29] Zatarain M, Ruiz de Argandoña I, Illarramendi a., Azpeitia JLL, Bueno R. New Control Techniques Based on State Space Observers for Improving the Precision and Dynamic Behaviour of Machine Tools. CIRP Ann - Manuf Technol 2005;54:393–6. doi:10.1016/S0007-8506(07)60130-9.
[30] Uriarte L, Zatarain M, Axinte D, Yagüe-Fabra J, Ihlenfeldt S, Eguia J, et al. Machine tools for large parts. CIRP Ann - Manuf Technol 2013;62:731–50. doi:10.1016/j.cirp.2013.05.009.
[31] Soemers H. Design Principles: For Precision Mechanisms. T-Pointprint; 2011.
[32] Leadbeater PB, Clarke M, Wills-Moren WJ, Wilson TJ. A unique machine for grinding large, off-axis optical components: the OAGM 2500. Precis Eng 1989;11:191–6. doi:10.1016/0141-6359(89)90028-7.
[33] Huo D, Cheng K, Wardle F. A holistic integrated dynamic design and modelling approach applied to the development of ultraprecision micro-milling machines. Int J Mach Tools Manuf 2010;50:335–43. doi:http://dx.doi.org/10.1016/j.ijmachtools.2009.10.009.
[34] Kurita T, Hattori M. Development of new-concept desk top size machine tool. Int J Mach Tools Manuf 2005;45:959–65. doi:10.1016/j.ijmachtools.2004.10.009.
[35] Brecher C, Utsch P, Klar R, Wenzel C. Compact design for high precision machine tools. Int J Mach Tools Manuf 2010;50:328–34. doi:http://dx.doi.org/10.1016/j.ijmachtools.2009.11.007.
[36] Shore P, Morantz P, Read R. Design overview of the μ4 Compact 6 axes ultra precision diamond machining centre. 10th Int. Conf. Exhib. Laser Metrol. Mach. Tool, C. Robot. Performance., euspen; 2013.
[37] Åström KJ, Hägglund T. The future of PID control. Control Eng Pract 2001;9:1163–75. doi:10.1016/S0967-0661(01)00062-4.
[38] Fleming AJ. A review of nanometer resolution position sensors: Operation and performance. Sensors Actuators, A Phys 2013;190:106–26. doi:10.1016/j.sna.2012.10.016.
[39] Gao W, Kim SW, Bosse H, Haitjema H, Chen YL, Lu XD, et al. Measurement technologies for precision positioning. CIRP Ann - Manuf Technol 2015;64:773–96. doi:10.1016/j.cirp.2015.05.009.
[40] Abir J, Longo S, Morantz P, Shore P. Optimized estimator for real-time dynamic displacement measurement using accelerometers. Mechatronics 2016;39:1–11. doi:10.1016/j.mechatronics.2016.07.003.
[41] Thong YK, Woolfson MS, Crowe JA, Hayes-Gill BR, Jones DA. Numerical double integration of acceleration measurements in noise. Meas J Int Meas Confed 2004;36:73–92. doi:10.1016/j.measurement.2004.04.005.
[42] Abir J, Morantz P, Longo S, Shore P. Feedback based technique for improving dynamic performance of a small size machine tool. ASPE 2016 Spring Top. Meet. Precis. Mechatron. Syst. Des. Control, American Society for Precision Engineering, ASPE; 2016, p. 58–61.
[43] Abir J, Morantz P, Longo S, Shore P. An accelerometer based-feedback technique for improving dynamic performance of a machine tool. Proc. 16th Int. Conf. Eur. Soc. Precis. Eng. Nanotechnol., 2016, p. 197–8.
[44] Celik O, Gilbert HB, O'Malley MK. Dynamic displacement sensing, system identification, and control of a speaker-based tendon vibrator via accelerometers. IEEE/ASME Trans Mechatronics 2013;18:812–7. doi:10.1109/TMECH.2012.2195326.
[45] Spiewak S, Zaiss C, Ludwick SJ. High Accuracy, Low-Invasive Displacement Sensor (HALIDS). Proc. ASME 2013 Int. Mech. Eng. Congr. Expo., ASME; 2013, p. 77. doi:10.1115/IMECE2013-66767.
[46] Abir J, Shore P, Morantz P. Influence of temperature changes on a linear motion system. Laser Metrol. Mach. Perform. XI - 11th Int. Conf. Exhib. Laser Metrol. Mach. Tool, C. Robot. Performance, LAMDAMAP 2015, euspen; 2015, p. 126–35.
[47] RENISHAW PLC. Tonic incremental encoder 2015. http://www.renishaw.com/en/tonic-incremental-encoder-system-

with-rslm-linear-scale--10242 (accessed August 17, 2015).
[48] Abir J, Shore P, Morantz P. System identification of a small size machine. Proc. 12th Int. Conf. Manuf. Res. (ICMR 2014), 2014, p. 35–40.
[49] Abir J, Morantz P, Shore P. Position errors due to structural flexible modes. Proc. 15th Int. Conf. Eur. Soc. Precis. Eng. Nanotechnol., 2015, p. 219–20.
[50] Levinzon FA. Fundamental Noise Limit of Piezoelectric Accelerometer. IEEE Sens J 2004;4:108–11. doi:10.1109/JSEN.2003.820366.
[51] Gross H, Wiegartner G, Hamann J. Electrical Feed Drives in Automation: Basics, Computation, Dimensioning. John Wiley & Sons, Inc.; 2001.
[52] Younkin GW. Industrial Servo Control Systems: Fundamentals And Applications, Revised And Expanded. CRC Press; 2002.
[53] Apkarian P, Noll D. Nonsmooth H_infty Synthesis. IEEE Trans Automat Contr 2006;51:71–86. doi:10.1109/TAC.2005.860290.
[54] Bruinsma NA, Steinbuch M. A fast algorithm to compute the of a transfer function matrix. Syst Control Lett 1990;14:287–93. doi:10.1016/0167-6911(90)90049-Z.
[55] Ewins DJ. Modal testing: theory, practice and application, 2000. Res Stud Press LTD, Baldock, Hertfordshire, Engl n.d.;171:415–37.
[56] Franklin G, Powell J, Emami-Naeini A. Feedback Control of Dynamics Systems. Reading, MA: 2015.
[57] Munnig Schmidt R, Schitter G, van Eijk J. The design of high performance mechatronics. 2nd ed. IOS Press; 2014.